Journal of Contaminant Hydrology 120–121 (2011) 129–140

Contents lists available at ScienceDirect

Journal of Contaminant Hydrology

journal homepage: www.elsevier.com/locate/jconhyd

PDF equations for advective–reactive transport in heterogeneous porous media with uncertain properties ☆

Daniel M. Tartakovsky *, Svetlana Broyda

Department of Mechanical and Aerospace Engineering, University of California, San Diego, 9500 Gilman Drive, La Jolla, CA 92093, USA

ARTICLE INFO

Article history:
Received 29 November 2009
Received in revised form 16 August 2010
Accepted 27 August 2010
Available online 21 September 2010

Keywords:
Reactive transport
Uncertainty quantification
Heterogeneous reaction
Stochastic modeling
Geochemistry
Random

ABSTRACT

We consider advective–reactive solute transport in porous media whose hydraulic and transport properties are uncertain. These properties are treated as random fields, which renders nonlinear advection–reaction transport equations stochastic. We derive a deterministic equation for the probability density function (PDF) of the concentration of a solute that undergoes heterogeneous reactions, e.g., precipitation or dissolution. The derivation treats exactly (without linearization) a reactive term in the transport equation which accounts for uncertainty (randomness) in both flow velocity and kinetic rate constants but requires a closure, such as a Large-Eddy-Diffusivity (LED) approximation used in the present analysis. No closure is required when reaction rates are the only source of uncertainty. We use exact concentration PDFs obtained for this setting to analyze the accuracy of our general, LED-based PDF equations.

© 2010 Elsevier B.V. All rights reserved.

1. Introduction

Proper modeling of physical and chemical processes involved in subsurface transport of reactive solutes requires quantification of uncertainty about hydraulic and transport properties of porous media. This is because subsurface environments are inherently heterogeneous on multiple scales and typically under-characterized by data. Such parametric uncertainty can be quantified by treating relevant properties, e.g., hydraulic conductivity $K(\mathbf{x})$ and kinetic rate constant $\kappa(\mathbf{x})$, as random fields whose spatial (and, by inference, ensemble) statistics are estimated from available data (Dagan, 1989; Gelhar, 1993; Cushman, 1997; Dagan and Neuman, 1997). This renders system states, e.g., hydraulic head h, macroscopic flux $\mathbf{q}$ and solute concentration c, random as well. Corresponding flow and transport equations become stochastic.

Most stochastic analyses of flow and transport in (randomly) heterogeneous porous media employ either Monte Carlo simulations (MCS) or moment differential equations (MDEs). The MCS approach consists of generating a sufficiently large number of realizations of random system parameters (e.g., conductivity and/or reaction rates), solving the corresponding flow and transport equations for each realization of parameters, and obtaining statistics for the system states (e.g., mean and variance of hydraulic head and solute concentration). While conceptually straightforward, MCS have a number of potential drawbacks. For nonlinear systems, especially those involving transient multi-component reactive transport in three spatial dimensions, MCS often prove to be computationally prohibitive and lack well-established criteria for their convergence. Additionally, MCS provide little or no physical insight into computed moments of system states. (More recently, various flavors of stochastic finite elements, e.g., polynomial chaos expansions and stochastic collocation on sparse grids, have found their way into subsurface hydrology (Xiu and Tartakovsky, 2004; Lin and Tartakovsky, 2009; Foo and Karniadakis, 2010). Under

☆ This research was supported by the DOE Office of Science Advanced Scientific Computing Research (ASCR) program in Applied Mathematical Sciences, and by the Office of Science (BER), Cooperative Agreement No. DE-FC02-07ER64324.

* Corresponding author. Tel.: +505 667 0968; fax: +505 665 5757.
E-mail address: dmt@ucsd.edu (D.M. Tartakovsky).

0169-7722/$ – see front matter © 2010 Elsevier B.V. All rights reserved.
doi:10.1016/j.jconhyd.2010.08.009

certain conditions, such approaches can be computationally more demanding than MCS (e.g., Foo and Karniadakis, 2010; and Xiu and Tartakovsky, 2006, Sec. 3.3.3; and the references therein).

MDEs can be used to alleviate some of these limitations by deriving deterministic equations for ensemble moments – typically, mean and (co)variance – of system states. Their applications to transport of solutes undergoing linear (first-order) chemical reactions include Bellin et al. (1993), Cushman et al. (1995), Cvetkovic et al. (1999), Severino et al. (2006), among many others. For nonlinear reaction rates, this approach entails linearization of the reactive terms, e.g., Simmons et al. (1995) and Ginn et al. (2001), which introduces uncontrollable errors that might compromise the robustness and accuracy of resulting solutions. Except under very special circumstances (e.g., one-dimensional flow and/or transport), MDEs require a closure approximation, such as perturbation expansions (Neuman and Tartakovsky, 2009 and references therein) or the assumption of Gaussianity of macroscopic flow velocity (Darcian flux) (Dentz and Tartakovsky, 2008). These and other closures limit the range of applicability of such analyses. For example, MDEs based on perturbation expansions are formally limited to mildly heterogeneous porous media. Moreover, since MDEs yield only the first few statistical moments of system states, they are suboptimal for predicting rare events, probabilistic risk assessment, and decision-making under uncertainty (Tartakovsky, 2007; Winter and Tartakovsky, 2008; Bolster et al., 2009).

Methods based on deriving deterministic differential equations for probability density functions (PDFs) of system states directly address the latter shortcoming. As an added benefit, they do not require linearization of reactive terms in transport equations. PDF methods have originally been developed to study turbulence and combustion (e.g., Pope, 1981, 2000; and the references therein), where it is common to assume that flow domains are infinite, random flow velocities are statistically homogeneous (stationary) and Gaussian, and reaction rates are deterministic constants. Virtually none of these assumptions hold in applications to reactive transport in porous media. In particular, reaction rates are often the main source of uncertainty since they depend heavily on pore geometry (Lichtner and Tartakovsky, 2003).

Quantification of uncertainty for such reactive flows is the main goal of our analysis. In previous studies (Tartakovsky et al., 2009; Broyda et al., 2010), PDFs for advective–reactive transport were derived by assuming that a porous medium is chemically heterogeneous but hydraulically homogeneous, i.e., by treating macroscopic flow velocity as deterministic (certain) and reaction rate constants as random (uncertain). The analysis below accounts for uncertainty (randomness) in both flow velocity reaction rates. We start by formulating in Section 2 governing equations for advective–reactive transport in porous media. Section 3 contains a derivation of PDF equations, which relies on a Large-Eddy-Diffusivity (LED) closure. Numerical solutions of these PDF equations are presented in Section 4 for linear (Section 4.1) and nonlinear (Section 4.2) heterogeneous reactions. These numerical solutions deal with transport phenomena in which reaction rates are the sole source of uncertainty. Such a setting enables us to validate the LED closure by comparing a corresponding equation for the PDF of concentration with its exact counterpart developed in Tartakovsky et al. (2009) (Section 4.3).

2. Problem formulation

Consider reactive transport in a porous medium Ω involving a heterogeneous reaction between a dissolved species $\mathcal{C}$ and a solid $\mathcal{C}_{(s)}$,

$$\alpha\mathcal{C} \rightleftharpoons \mathcal{C}_{(s)}, \tag{1}$$

in steady-state (divergence-free) groundwater flow with macroscopic velocity $\mathbf{v}$. For a given stoichiometric coefficient α, the speed with which the concentration c of $\mathcal{C}$ reaches its equilibrium level C_{eq} is determined by the kinetic rate constant (Tartakovsky et al., 2009)

$$\kappa = \frac{k_0 A C_{\mathrm{eq}}^{-\alpha}}{\phi}. \tag{2}$$

The latter represents the product of the laboratory measured kinetic rate constant k_0 [mol $L^{-2}T^{-1}$] for reaction (1) and the specific surface area A [L^{-1}] of a porous matrix. In this definition, the kinetic rate constant κ [$(\mathrm{mol\ L^{-3}})^{1-\alpha}T^{-1}$] includes the contribution from the specific surface area A and porosity ϕ, both of which are assumed to be constant in time. Following Neuman (1993), Shvidler and Karasaki (2003) and many others, we neglect diffusion and hydrodynamic dispersion on a local scale ω, i.e., assume that mixing in the aqueous phase does not control reactions. Then the evolution of the solute concentration $c(\mathbf{x},t)$ can be described by an advection–reaction equation (ARE)

$$\frac{\partial c}{\partial t} = -\nabla\cdot(\mathbf{v}c) + f_\kappa(c), \quad \mathbf{x}\in\Omega. \tag{3}$$

The source function

$$f_\kappa(c) = -\kappa\alpha(c^\alpha - C_{\mathrm{eq}}^\alpha) \tag{4}$$

provides a macroscopic (continuum-scale) representation of the heterogeneous precipitation/dissolution reaction (1). It is worthwhile emphasizing that the methodology described below is applicable to other types of chemical reactions.

Equation (3) is subject to the initial condition

$$c(\mathbf{x},0) = C_0(\mathbf{x}) \tag{5}$$

where the initial distribution C_0 can be either certain (deterministic) or uncertain (random).

Spatial heterogeneity and scarcity of data render both $\mathbf{v}(\mathbf{x})$ and $\kappa(\mathbf{x})$ uncertain. To quantify the impact of this uncertainty of predictions of concentration $c(\mathbf{x},t)$, we treat $\mathbf{v}(\mathbf{x})$ and $\kappa(\mathbf{x})$ as random fields. The data discussed in Tartakovsky et al. (2009) and Broyda et al. (2010) suggest that the reaction rate constant $\kappa(\mathbf{x})$ can be modeled as a statistically homogeneous multi-variate lognormal filed with mean $\langle\kappa\rangle$ and two-point covariance $C_\kappa(|\mathbf{x}-\mathbf{y}|)$. Statistics of macroscopic flow velocity $\mathbf{v}(\mathbf{x})$, including its spatially varying mean $\langle\mathbf{v}(\mathbf{x})\rangle$ and covariance $C_{v_{ij}}(\mathbf{x},\mathbf{y})$ $(i,j=1,2,3)$, are determined by solving flow

equations with uncertain hydraulic conductivity. The stoichiometric coefficient α, the equilibrium concentration C_{eq}, and porosity ϕ are assumed to be deterministic.

The advection–reaction problem (3)–(5) is defined on a local scale ω that is larger than the pore scale but smaller than field-scale variations in physical properties, including macroscopic flow velocity. The latter allows one to disregard local dispersion in (3). The mesoscale transport equation breaks down when the reaction rate $f_\kappa(c)$ becomes large enough to produce gradients on the scale of a single pore diameter (Battiato et al., 2011-this issue; Kechagia et al., 2002). In such cases it is necessary to explicitly account for diffusion-controlled reaction at the surface of the solid by means of either pore-scale (Tartakovsky et al., 2007a, 2008) or hybrid (Tartakovsky et al., 2007b) simulations.

Direct stochastic averaging of (3), e.g., Simmons et al. (1995) and Ginn et al. (2001), requires one to expand the nonlinear source term $f_\kappa(c)$ into a Taylor series about mean concentration $\langle c(\mathbf{x},t)\rangle$,

$$f_\kappa(c) = f_\kappa(\langle c\rangle) + c'\frac{df_\kappa}{dc}(\langle c\rangle) + \frac{c'^2}{2}\frac{d^2 f_\kappa}{ds^2}(\langle c\rangle) + \dots \tag{6}$$

where $c'(\mathbf{x},t)$ are the zero-mean random fluctuations of c around its mean $\langle c\rangle$, such that $c=\langle c\rangle + c'$. Retaining the leading term in (6) leads to linearized solutions, which are clearly inexact. Retaining higher-order terms gives rise to rigorous perturbation solutions. Either approach is insufficient for conditions far from equilibrium, $c \gg C_{eq}$ or $c \ll C_{eq}$, which compromise the convergence of the Taylor series (6). The probability density function (PDF) approach presented in Section 3 does not require the expansion (6).

2.1. Non-dimensional formulation

The subsequent analysis is facilitated by rewriting the advection–reaction problem (3)–(5) in its dimensionless form. Let t_a denote an advection time scale defined as the time it takes a solute to travel a characteristic length L of the physical domain with a characteristic macroscopic velocity V,

$$t_a = \frac{L}{V}. \tag{7}$$

Let t_r denote a reaction time scale defined by

$$t_r = \frac{C_{eq}^{1-\alpha}}{\langle\kappa\rangle}. \tag{8}$$

Then the relative importance of advection and reactions can be quantified in terms of the dimensionless Damköhler number $\mathrm{Da}=t_a/t_r$ as

$$\mathrm{Da} = \frac{L\langle\kappa\rangle}{V}C_{eq}^{\alpha-1}. \tag{9}$$

Introducing dimensionless quantities

$$\hat{\mathbf{x}} \equiv \frac{\mathbf{x}}{L},\ \hat{t} \equiv \frac{t}{t_a},\ \hat{\kappa} \equiv \frac{\kappa}{\langle\kappa\rangle},\ \hat{\mathbf{v}} \equiv \frac{\mathbf{v}}{V},\ \hat{c} \equiv \frac{c}{C_{eq}},\ \hat{C}_0 \equiv \frac{C_0}{C_{eq}}, \tag{10}$$

we transform (3)–(5) into their dimensionless form

$$\frac{\partial \hat{c}}{\partial \hat{t}} = -\hat{\nabla}\cdot(\hat{\mathbf{v}}\hat{c}) + \mathrm{Da}\hat{f}_\kappa(\hat{c}),\ \hat{f}_\kappa(\hat{c}) = -\alpha\hat{\kappa}(\hat{c}^\alpha - 1),$$
$$\hat{c}(\hat{\mathbf{x}},0) = \hat{C}_0(\hat{\mathbf{x}}). \tag{11}$$

It follows from (7)–(9) that the dimensionless advection time scale is $\hat{t}_a \equiv t_a/t_a = 1$ and the dimensionless reaction time scale is $\hat{t}_r \equiv t_r/t_a = \mathrm{Da}^{-1}$. We drop the hats $\hat{}$ to simplify the subsequent presentation.

3. PDF approach

Following Pope (1981), we consider a function

$$\Pi(c,C;\mathbf{x},t) \equiv \delta[c(\mathbf{x},t) - C] \tag{12}$$

where $\delta(\cdot)$ is the Dirac delta function and C is a deterministic value the random concentration c can take on at a space–time point $(\mathbf{x},t)$. The ensemble average (over random c) of Π is the one-point PDF for concentration $c(\mathbf{x},t)$,

$$p(C;\mathbf{x},t) = \langle\Pi(c,C;\mathbf{x},t)\rangle. \tag{13}$$

An equation for $p(C;\mathbf{x},t)$ is derived by noting that

$$\frac{\partial\Pi}{\partial t} = \frac{\partial\Pi}{\partial c}\frac{\partial c}{\partial t} = -\frac{\partial\Pi}{\partial C}\frac{\partial c}{\partial t}, \tag{14a}$$

$$\nabla\cdot(\mathbf{v}\Pi) = \frac{\partial \mathbf{v}\Pi}{\partial c}\cdot\nabla c = -\frac{\partial\Pi}{\partial C}\mathbf{v}\cdot\nabla c, \tag{14b}$$

and

$$f_\kappa(c)\frac{\partial\Pi}{\partial C} = \frac{\partial}{\partial C}[f_\kappa(c)\Pi] \equiv \frac{\partial}{\partial C}[f_\kappa(c)\delta(c-C)] = \frac{\partial}{\partial C}[f_\kappa(C)\Pi]. \tag{14c}$$

Substituting (14) into (3) yields

$$\frac{\partial\Pi}{\partial t} + \nabla\cdot(\mathbf{v}\Pi) = -\mathrm{Da}\frac{\partial f_\kappa(C)\Pi}{\partial C}. \tag{15}$$

Let us introduce a four-dimensional space $\tilde{\mathbf{x}} = (x_1, x_2, x_3, x_4 \equiv C)^T$, in which the gradient and "velocity" are defined as

$$\tilde{\nabla} \equiv \left(\frac{\partial}{\partial x_1}, \frac{\partial}{\partial x_2}, \frac{\partial}{\partial x_3}, \frac{\partial}{\partial x_4} \equiv \frac{\partial}{\partial C}\right)^T,\ \tilde{\mathbf{v}} = (v_1, v_2, v_3, v_4 \equiv \mathrm{Da}f_\kappa)^T. \tag{16}$$

Then (15) can be written in the form of an advection equation,

$$\frac{\partial\Pi}{\partial t} = -\tilde{\nabla}\cdot(\tilde{\mathbf{v}}\Pi),\ \ \tilde{\mathbf{x}} \in \tilde{\Omega} \equiv \Omega\times(C_0,1), \tag{17}$$

which describes the spreading of Π in the random velocity field $\tilde{\mathbf{v}}$. (It is worthwhile recognizing that the velocity field $\tilde{\mathbf{v}}$ is no-longer divergence-free. Instead, $\tilde{\nabla}\cdot\tilde{\mathbf{v}} = \mathrm{Da}df_\kappa/dx_4$.)

Stochastic averaging of advective transport equations with random velocity has been the subject of numerous studies, e.g., Neuman (1993), Shvidler and Karasaki (2003)

and references therein. Most approaches start by employing the Reynolds decomposition, $\mathcal{A} = \langle\mathcal{A}\rangle + \mathcal{A}'$, to represent the random quantities in (17) as the sum of their ensemble means $\langle\mathcal{A}\rangle$ and zero-mean fluctuations about the mean $\mathcal{A}'$. Then, taking the ensemble average of (17) yields an equation for the concentration PDF,

$$\frac{\partial p}{\partial t} = -\tilde{\nabla}\cdot(\langle\tilde{\mathbf{v}}\rangle p) - \tilde{\nabla}\cdot\langle\tilde{\mathbf{v}}'\Pi'\rangle. \tag{18}$$

This equation contains the unknown cross-correlation term $\langle\tilde{\mathbf{v}}'\Pi'\rangle$ and, hence, requires a closure approximation. Over the years, a plethora of closures for $\langle\tilde{\mathbf{v}}'\Pi'\rangle$ have been proposed. These include closures based either on physical arguments, e.g., the "direct interaction approximation" (Kraichnan, 1965), the "weak approximation" (Neuman, 1993), and a four-point closure (Dentz and Tartakovsky, 2008) or on approximations based on perturbation expansions in the (small) variance of velocity fluctuations (Winter et al., 1984; Dagan, 1989). For time-dependent problems similar to (18), perturbation expansions often prove to be divergent (Frisch, 1968; Jarman and Tartakovsky, 2008; Tartakovsky et al., 2009). We therefore adopt a phenomenological closure, which gives rise to a diffusive term called macro-dispersion.

3.1. Large-Eddy-Diffusivity (LED) approximation

Let us introduce a random Green's function $\mathcal{G}(\tilde{\mathbf{x}}, \tilde{\mathbf{y}}, t-\tau)$ associated with (17). It is defined as a solution of

$$\frac{\partial \mathcal{G}}{\partial \tau} + \tilde{\mathbf{v}}\cdot\tilde{\nabla}_{\tilde{\mathbf{y}}}\mathcal{G} = -\delta(\tilde{\mathbf{x}}-\tilde{\mathbf{y}})\delta(t-\tau) \tag{19}$$

subject to the homogeneous boundary and initial conditions. Then (18) can be approximated by (Appendix A)

$$\frac{\partial p}{\partial t} = -\frac{\partial \tilde{u}_i p}{\partial \tilde{x}_i} + \frac{\partial}{\partial \tilde{x}_j}\left[\tilde{D}_{ij}\frac{\partial p}{\partial \tilde{x}_i}\right], \tag{20}$$

where the Einstein notation is used to indicate the summation over the repeated indices. Components of the eddy-diffusivity (macro-dispersion) tensor $\tilde{D}_{ij}(\tilde{\mathbf{x}}, t)$ are given by

$$\tilde{D}_{ij}(\tilde{\mathbf{x}}, t) = \int_0^t \int_{\tilde{\Omega}} \langle \tilde{v}_i'(\tilde{\mathbf{x}})\tilde{v}_j'(\tilde{\mathbf{y}})\mathcal{G}(\tilde{\mathbf{x}}, \tilde{\mathbf{y}}, t-\tau)\rangle \, \mathrm{d}\tilde{\mathbf{y}}\mathrm{d}\tau, i,j = 1,\ldots,4. \tag{21}$$

This result is asymptotically exact if p varies slowly in time and hyperspace $\tilde{\Omega}$ relative to $\tilde{\mathbf{v}}$ (Kraichnan, 1987). The effective velocity $\tilde{\mathbf{u}}$ is given by

$$\tilde{\mathbf{u}} = \langle\tilde{\mathbf{v}}\rangle - \mathrm{Da}\int_0^t \int_{\tilde{\Omega}} \langle \tilde{\mathbf{v}}'(\tilde{\mathbf{x}})\frac{\mathrm{d}f_\kappa'(\tilde{\mathbf{y}})}{\mathrm{d}y_4}\mathcal{G}\rangle \mathrm{d}\tilde{\mathbf{y}}\mathrm{d}\tau. \tag{22}$$

Following Neuman (1993) and many others, we approximate (21) and (22) by

$$\tilde{D}_{ij}(\tilde{\mathbf{x}}, t) \approx \int_0^t \int_{\tilde{\Omega}} \langle \tilde{v}_i'(\tilde{\mathbf{x}})\tilde{v}_j'(\tilde{\mathbf{y}})\rangle \, G(\tilde{\mathbf{x}}, \tilde{\mathbf{y}}, t-\tau)\mathrm{d}\tilde{\mathbf{y}}\mathrm{d}\tau \tag{23}$$

and

$$\tilde{\mathbf{u}} \approx \langle\tilde{\mathbf{v}}\rangle - \mathrm{Da}\int_0^t \int_{\tilde{\Omega}} \langle \tilde{\mathbf{v}}'(\tilde{\mathbf{x}})\kappa'(\mathbf{y})\rangle \frac{\mathrm{d}\mathbf{f}_\alpha}{\mathrm{d}\mathbf{y}_4}\mathbf{G}(\tilde{\mathbf{x}}, \tilde{\mathbf{y}}, \mathbf{t}-\tau)\mathrm{d}\tilde{\mathbf{y}}\mathrm{d}\tau, \tag{24}$$

respectively. Here $f_\alpha(x_4) \equiv -\alpha(x_4^\alpha - 1)$, and $G(\tilde{\mathbf{x}}, \tilde{\mathbf{y}}, t-\tau)$ is the deterministic Green's function defined as a solution of

$$\frac{\partial G}{\partial \tau} + \langle\tilde{\mathbf{v}}\rangle\cdot\tilde{\nabla}_{\tilde{\mathbf{y}}}G = -\delta(\tilde{\mathbf{x}}-\tilde{\mathbf{y}})\delta(t-\tau) \tag{25}$$

subject to the corresponding homogeneous boundary and initial conditions.

Deterministic advection–dispersion Eq. (20) with effective "velocity" $\tilde{\mathbf{u}}$ in (24) and "macro-dispersion" coefficient $\tilde{\mathbf{D}}$ in (23) describes the evolution of the concentration PDF $p(C; \mathbf{x}, t)$. These results are valid for an arbitrary degree of correlation between macroscopic velocity $\mathbf{v}(\mathbf{x})$ and reaction rate constant $\kappa(\mathbf{x})$.

If $\mathbf{v}(\mathbf{x})$ and $\kappa(\mathbf{x})$ are mutually uncorrelated, then the components of the covariance tensors in (23) and (24) reduce to

$$\langle \tilde{v}_i'(\tilde{\mathbf{x}})\tilde{v}_j'(\tilde{\mathbf{y}})\rangle = \langle v_i'(\mathbf{x})v_j'(\mathbf{y})\rangle \equiv C_{v_{ij}}(\mathbf{x}, \mathbf{y}), \quad i,j = 1,2,3, \tag{26a}$$

$$\langle \tilde{v}_4'(\tilde{\mathbf{x}})\tilde{v}_4'(\tilde{\mathbf{y}})\rangle = \mathrm{Da}^2 C_\kappa(\mathbf{x}, \mathbf{y}) f_\alpha(x_4) f_\alpha(y_4), \tag{26b}$$

and

$$\mathbf{u} = \langle\mathbf{v}\rangle, \quad u_4 \approx \mathrm{Da}f_\alpha - \mathrm{Da}^2 f_\alpha \int_0^t \int_{\tilde{\Omega}} C_\kappa(\mathbf{x}, \mathbf{y})\frac{\mathrm{d}f_\alpha}{\mathrm{d}y_4} G(\tilde{\mathbf{x}}, \tilde{\mathbf{y}}, t-\tau)\mathrm{d}\tilde{\mathbf{y}}\mathrm{d}\tau, \tag{27}$$

respectively. Here $C_\kappa(\mathbf{x}, \mathbf{y})$ is a two-point covariance of the reaction rate constant $\kappa(\mathbf{x})$.

3.2. Auxiliary conditions for the PDF Eq. (20)

An initial condition for $p(\tilde{\mathbf{x}}, t) \equiv p(C; \mathbf{x}, t)$ in (20),

$$p(C; \mathbf{x}, 0) = p_{\mathrm{in}}(C; \mathbf{x}), \tag{28}$$

is determined by the degree of uncertainty in the initial concentration $C_0(\mathbf{x})$ in (5), i.e., by its PDF $p_{\mathrm{in}}(C; \mathbf{x})$. If the knowledge of $C_0(\mathbf{x})$ is perfect, i.e., if $C_0(\mathbf{x})$ is deterministic, then

$$p(C; \mathbf{x}, 0) = p_{\mathrm{in}}(C; \mathbf{x}) = \delta[C - C_0(\mathbf{x})]. \tag{29}$$

The boundary conditions $p(C; \mathbf{x} \in \partial\Omega, t)$ along the boundaries $\partial\Omega$ of the flow domain Ω are determined by the probabilistic distributions of the boundary conditions for the concentration $c(\mathbf{x}, t)$ on $\mathbf{x} \in \partial\Omega$.

Derivation of unique boundary conditions for $p(C; \mathbf{x}, t)$ at $C = C_0$ and $C = 1$ remains an open question. In Section 4, we derive such conditions for reactive transport in heterogeneous porous media in which reaction rate constant $\kappa(\mathbf{x})$ is the only source of uncertainty (macroscopic flow velocity field is certain and, hence, deterministic).

Finally, a solution of (20) is subject to the constraint

$$\int_{C_0}^{1} p(C;\mathbf{x},t)\mathrm{d}C = 1 \quad \text{or} \quad \int_{1}^{C_0} p(C;\mathbf{x},t)\mathrm{d}C = 1, \quad \forall \mathbf{x},t, \tag{30}$$

where the order of limits of integration depends on whether the initial concentration C_0 is smaller or grater than the equilibrium concentration C_{eq}, respectively.

4. Computational examples

To demonstrate the salient features of the proposed PDF approach, we consider reactive transport in heterogeneous porous media in which reaction rate constant $\kappa(\mathbf{x})$ is the only source of uncertainty (macroscopic flow velocity field $\mathbf{v}(\mathbf{x})$ is certain and, hence, deterministic). Such a setting lends itself to an exact semi-analytical treatment (Tartakovsky et al., 2009; Broyda et al., 2010) and, therefore, can be used to analyze errors introduced by the approximations leading to the PDF Eq. (20). For $v_i'(\mathbf{x})\equiv 0$ $(i=1,2,3)$, the only non-zero component of the "macro-dispersion" tensor (23) is

$$D_{44} \approx \mathrm{Da}^2 f_\alpha(x_4) \int_0^t \int_{\tilde{\Omega}} C_\kappa(\mathbf{x},\mathbf{y}) f_\alpha(y_4) G(\tilde{\mathbf{x}},\tilde{\mathbf{y}},t-\tau)\mathrm{d}\tilde{\mathbf{y}}\mathrm{d}\tau, \tag{31}$$

and the PDF Eq. (20) reduces to

$$\frac{\partial p}{\partial t} = -\nabla\cdot(\mathbf{v}p) - \frac{\partial u_4 p}{\partial x_4} + \frac{\partial}{\partial x_4}\left[D_{44}\frac{\partial p}{\partial x_4}\right]. \tag{32}$$

Solution of the PDF Eq. (32) is facilitated by introducing a new dependent variable,

$$\mathcal{F}(x_4;\mathbf{x},t) = \int_{C_0}^{x_4} p(x_4';\mathbf{x},t)\mathrm{d}x_4' \text{ or } \mathcal{F}(x_4';\mathbf{x},t) = \int_{1}^{x_4} p(x_4;\mathbf{x},t)\mathrm{d}x_4', \tag{33}$$

for the dimensionless initial concentration C_0 smaller or larger than the dimensionless equilibrium concentration $C_{\mathrm{eq}}=1$, respectively. To be concrete, the subsequent examples correspond to the constant initial concentration $C_0=0$, so that the first definition of $\mathcal{F}$ will be used. Since $x_4\equiv C$, the new dependent variable $\mathcal{F}(C;\mathbf{x},t)$ represents a single-point cumulative distribution function (CDF) of concentration, which is defined as the probability that the random concentration c at space–time point $(\mathbf{x},t)$ does not exceed a deterministic value C, i.e., $\mathcal{F}(C;\mathbf{x},t)\equiv \Pr[c(\mathbf{x},t)\le C]$.

Integrating (32) over x_4 from $C_0=0$ to x_4 and using the definition of the CDF $\mathcal{F}(x_4;\mathbf{x},t)$ in (33), we obtain a CDF equation

$$\frac{\partial \mathcal{F}}{\partial t} = -\nabla\cdot(\mathbf{v}\mathcal{F}) - u_4\frac{\partial \mathcal{F}}{\partial x_4} + D_{44}\frac{\partial^2 \mathcal{F}}{\partial x_4^2}, \quad (\mathbf{x},x_4)\in\Omega\times(0,1). \tag{34}$$

An advantage of using the CDF Eq. (34) instead of the PDF Eq. (32) is that boundary conditions for the former are easier to define. Indeed, the definition of CDF, $\mathcal{F}(x_4;\mathbf{x},t)\equiv \Pr[c(\mathbf{x},t)\le x_4]$, imposes boundary conditions

$$\mathcal{F}(x_4=0;\mathbf{x},t)=0, \quad \mathcal{F}(x_4=1;\mathbf{x},t)=1, \quad \mathbf{x}\in\Omega, \quad t>0. \tag{35a}$$

The initial condition (29) translates into

$$\mathcal{F}(x_4;\mathbf{x},t=0)=1, \quad (\mathbf{x},x_4)\in\Omega\times(0,1). \tag{35b}$$

Boundary conditions for $\mathcal{F}(x_4;\mathbf{x},t)$ along the boundary $\partial\Omega$ of the flow domain Ω are determined by the corresponding boundary conditions for concentration $c(\mathbf{x},t)$.

By way of an example, let us consider one-dimensional flow in the x_1 direction (referred to below as x) in a semi-infinite domain $\Omega=[0,\infty)$. The non-dimensional macroscopic flow velocity is set to $v=1$. The dimensionless concentration at the flow inlet $x=0$ is $c(x=0,t)=0$, while at $x\to\infty$ ($x=250$ in numerical simulations) the equilibrium concentration is maintained, $c(x\to\infty,t)=1$. The corresponding boundary conditions for the concentration PDF $p(x_4;x,t)$,

$$p(x_4;0,t)=\delta(x_4), \quad p(x_4;\infty,t)=\delta(x_4-1), \quad x_4\in(0,1), \quad t>0, \tag{36}$$

give rise to the boundary conditions for the concentration CDF,

$$\mathcal{F}(x_4;0,t)=1, \quad \mathcal{F}(x_4;\infty,t)=0, \quad x_4\in(0,1), \quad t>0. \tag{37}$$

In the numerical simulations reported below, we truncate the infinite domain $0\le x<\infty$ at $x=250$, and replace the boundary conditions at $x\to\infty$ with boundary conditions $\partial p/\partial x=0$ and $\partial\mathcal{F}/\partial x=0$ at $x=250$. The rest of this section is devoted to solving the boundary-value problem (34)–(37) for linear ($\alpha=1$) and nonlinear ($\alpha=2$) heterogeneous reactions.

4.1. Linear heterogeneous reaction, $\alpha=1$

With the Green's function given by (B. 13) of Appendix B, the "dispersion" coefficient in (31) and the effective "velocity" in (27) become (Appendix C)

$$D_{44} = \mathrm{Da}^2(x_4-1)^2 \begin{cases} \int_0^t C_\kappa(x,x-T)\mathrm{e}^{2\mathrm{Da}T}\mathrm{d}T & \text{if } t\le t_* \\ \int_0^{t_*} C_\kappa(x,x-T)\mathrm{e}^{2\mathrm{Da}T}\mathrm{d}T & \text{if } t>t_* \end{cases} \tag{38}$$

and

$$u_4 = \mathrm{Da}(1-x_4) - \mathrm{Da}^2(x_4-1) \begin{cases} \int_0^t C_\kappa(x,x-T)\mathrm{e}^{\mathrm{Da}T}\mathrm{d}T & \text{if } t\le t_* \\ \int_0^{t_*} C_\kappa(x,x-T)\mathrm{e}^{\mathrm{Da}T}\mathrm{d}T & \text{if } t>t_*, \end{cases} \tag{39}$$

where

$$t_* = \frac{1}{\mathrm{Da}} \ln\left(\frac{1}{1-x_4}\right). \tag{40}$$

We are now in a position to explore how the coefficients D_{44} and u_4 and, hence, the evolution of predictive uncertainty (the concentration CDF $\mathcal{F}$) are affected by C_κ, the spatial correlation of reaction rate constant $\kappa(x)$.

4.1.1. White-noise correlation function

We start by considering random reaction rate constants $\kappa(x)$ that lack spatial correlations,

$$C_\kappa(x,y) = \sigma_\kappa^2 \delta(x-y). \tag{41}$$

This correlation model was used by Tartakovsky et al., (2009) as a large-time approximation of a correlated $\kappa(x)$. Substituting (41) into (38) and (39) yields

$$D_{44} = \frac{\mathrm{Da}^2\sigma_\kappa^2}{2}(1-x_4)^2, \quad u_4 = \mathrm{Da}\left(1 + \frac{\mathrm{Da}\sigma_\kappa^2}{2}\right)(1-x_4), \tag{42}$$

The CDF Eq. (34) with the coefficients (42), subject to the initial and boundary conditions (35) and (37) was solved with a finite-difference discretization. The concentration PDF $p(C;x,t)$ was then computed via numerical differentiation of the computed CDF $\mathcal{F}(C;x,t)$ (recall that $x_4 \equiv C$). An outcome of these calculations is presented in Fig. 1 in the form of temporal snapshots of the concentration PDF.

Fig. 2 explores the dependence of the concentration PDF on the Damköhler number Da. The smaller the value of Da, the stronger the dominance of the dissolution reaction over advection. For $\mathrm{Da} = 10^{-3}$, the dimensionless concentration c $(x=50, t=25)$ is close to its deterministic initial value $C_0 = 0$, which corresponds to a sharply peaked PDF. For $\mathrm{Da} = 0.1$, the dimensionless concentration $c(x=50, t=25)$ approaches its deterministic equilibrium state $C_{\mathrm{eq}} = 0$, but the predictive uncertainty persists, manifesting itself in the long tail of a highly skewed PDF. For intermediate Da, the dimensionless concentration $c(x=50, t=25)$ is far from its deterministic bounds, giving rise to higher predictive uncertainty. While the concentration PDF for $\mathrm{Da} = 0.01$ is almost Gaussian, its counterpart for $\mathrm{Da} = 0.05$ is highly skewed. This suggests that the reliance on assumed concentration PDFs is problematic.

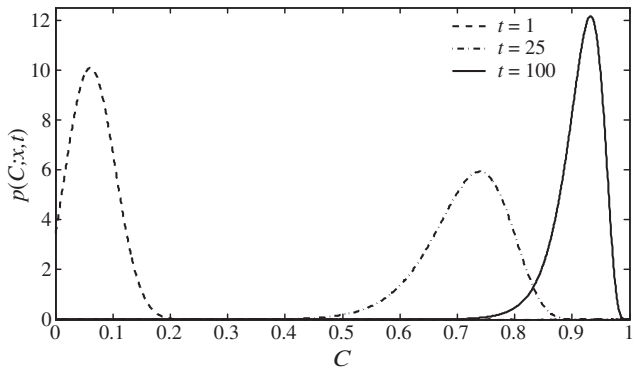

Fig. 1. Temporal evolution of the concentration PDF for the linear reaction law ($\alpha = 1$), spatially uncorrelated reaction rate constant $\kappa(x)$ and the following choice of parameters: $\mathrm{Da} = 0.05$ and $\sigma_\kappa^2 = 1$. Snapshots are calculated at point $x = 50$.

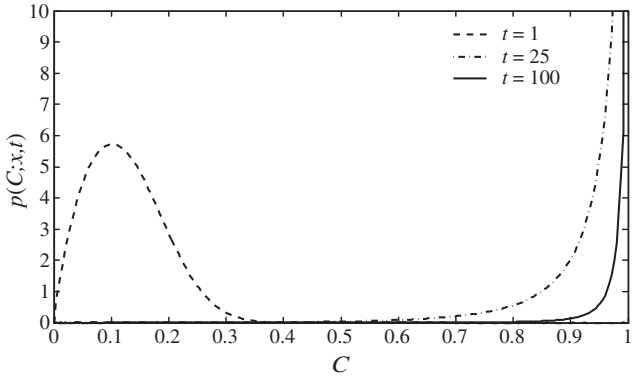

Fig. 2. The concentration PDF for the linear reaction law ($\alpha = 1$) with spatially uncorrelated reaction rate constant $\kappa(x)$ of variance $\sigma_\kappa^2 = 1$, computed at $x = 50$ and $t = 25$ for several values of Da.

4.1.2. Exponential correlation function

Next, we consider an exponential covariance function for kinetic rate constant $k(x)$,

$$C_\kappa(x,y) = \sigma_\kappa^2 \exp\left(-\frac{|x-y|}{\lambda_\kappa}\right), \tag{43}$$

where λ_κ is the dimensionless correlation length of κ, set to $\lambda_\kappa = 1$ in the subsequent numerical simulations. (One can think of the dimensional correlation length as a characteristic length of an infinite flow domain.) Substituting (43) into (38) and (39) yields

$$D_{44} = \frac{\mathrm{Da}^2\sigma_\kappa^2 (x_4-1)^2}{2\mathrm{Da}-1} \begin{cases} e^{(2\mathrm{Da}-1)t} - 1 & \text{if } t \le t_* \\ e^{(2\mathrm{Da}-1)t_*} - 1 & \text{if } t > t_* \end{cases} \tag{44}$$

and

$$u_4 = \mathrm{Da}(1-x_4) - \frac{\mathrm{Da}^2\sigma_\kappa^2 (x_4-1)}{\mathrm{Da}-1} \begin{cases} e^{(\mathrm{Da}-1)t} - 1 & \text{if } t \le t_* \\ e^{(\mathrm{Da}-1)t_*} - 1 & \text{if } t > t_* \end{cases}, \tag{45}$$

respectively.

The concentration PDF computed with numerical differentiation of the concentration CDF calculated as a finite-difference solution of (34) with the coefficients (44) and

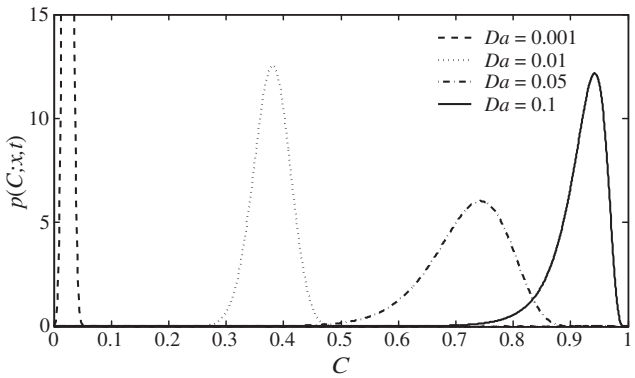

Fig. 3. Temporal evolution of the concentration PDF for the linear reaction law ($\alpha = 1$), exponentially correlated reaction rate constant $\kappa(x)$ and the following choice of parameters: $\mathrm{Da} = 0.05$, $\sigma_\kappa^2 = 1$, and $\lambda_p pa = 1$. Snapshots are calculated at point $x = 50$.

(45) is shown in Fig. 3. At early times, the PDF is close the delta function $\delta(0)$, reflecting the assumed certainty about the initial concentration $C_0 = 0$. At intermediate times, the concentration PDF is highly non-Gaussian, exhibiting non-symmetrical shapes and long tails. For large times, the PDF tends to the delta function $\delta(C-1)$ as the solute concentration reaches its deterministic equilibrium value. Comparison of Figs. 1 and 3 reveals that spatial correlations of the reaction rate constant $\kappa(x)$ reduce predictive uncertainty (result in more peaked concentration PDFs). This is to be expected, since the presence of correlations in input parameters provides additional information about their spatial variability.

4.2. Nonlinear reactions, $\alpha = 2$

With the Green's function given by (B.16) of Appendix B, the "dispersion" coefficient in (31) and the effective "velocity" in (27) become (Appendix C)

$$D_{44} = 64\mathrm{Da}^2 \begin{cases} \int_0^t C_\kappa(x, x-T)\,\dfrac{g^2\,\mathrm{d}T}{(g-1)^4} & \text{if } t \le t_* \\ \int_0^{t_*} C_\kappa(x, x-T)\,\dfrac{g^2\,\mathrm{d}T}{(g-1)^4} & \text{if } t > t_* \end{cases} \tag{46}$$

and

$$u_4 = -2\mathrm{Da}\left(x_4^2-1\right) - 32\mathrm{Da}^2 \begin{cases} \int_0^t C_\kappa(x, x-T)\,\dfrac{g(g+1)}{(g-1)^3}\,\mathrm{d}T & \text{if } t \le t_* \\ \int_0^{t_*} C_\kappa(x, x-T)\,\dfrac{g(g+1)}{(g-1)^3}\,\mathrm{d}T & \text{if } t > t_* \end{cases}, \tag{47}$$

where

$$t_* = \frac{1}{4\mathrm{Da}}\ln\left(\frac{1+x_4}{1-x_4}\right), \quad g(x_4, T) = \frac{x_4+1}{x_4-1}e^{-4\mathrm{Da}T}. \tag{48}$$

4.2.1. White-noise correlation function

For spatially uncorrelated random field κ, substituting (41) into (46) and (47) gives

$$D_{44} = 2\mathrm{Da}^2\sigma_\kappa^2\left(x_4^2-1\right)^2, \quad u_4 = 2\mathrm{Da}(1-x_4^2)(1+2\mathrm{Da}\sigma_\kappa^2 x_4). \tag{49}$$

The finite-difference solution of the resulting CDF equation and its subsequent numerical differentiation leads to the concentration PDFs shown in Fig. 4. Comparison of this figure with Fig. 1 shows that the effect of nonlinearity of the dissolution reaction is to speed up the transition to equilibrium, which decreases the time interval over which predictive uncertainty is significant. This is manifested in the sharp (nearly δ-like) PDF profile at $t = 100$.

4.2.2. Exponential correlation function

For the covariance function (43), the quadratures in the expressions for the "macro-dispersion" coefficient (46) and the effective "velocity" (47) were computed numerically. The resulting PDF profiles are shown in Fig. 5. Comparison of Figs. 4 and 5 confirms our earlier finding that the absence of spatial correlations of the reaction rate constant $\kappa(x)$ enhances the predictive uncertainty for solute concentration. Comparison of Figs. 3 and 5 demonstrates that the nonlinearity decreases the time interval over which predictive uncertainty is significant.

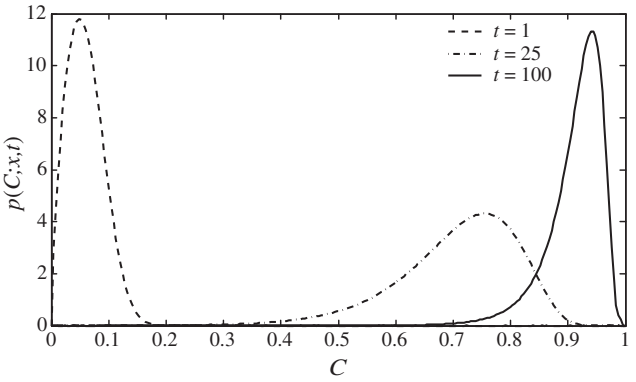

Fig. 4. Temporal evolution of the concentration PDF for the nonlinear reaction law with $\alpha = 2$, spatially uncorrelated reaction rate constant $\kappa(x)$ and the following choice of parameters: $\mathrm{Da} = 0.05$ and $\sigma_\kappa^2 = 1$. Snapshots are calculated at point $x = 50$.

4.3. Comparison with exact PDF equations

Concentration PDFs for reactive transport with constant flow velocity $\mathbf{v}$ and uncorrelated reaction rate constant $\kappa(\mathbf{x})$ satisfy *exactly* the Fokker–Planck equation (Tartakovsky et al., 2009, Eq. 26).

$$\frac{\mathrm{D}p}{\mathrm{D}t} = -\frac{\partial u_{\mathrm{exp}}}{\partial x_4} + \frac{\partial}{\partial x_4}\left(D_{\mathrm{ex}}\frac{\partial p}{\partial x_4}\right), \tag{50}$$

where $\mathrm{D}/\mathrm{D}t = \partial/\partial t + \mathbf{v}\cdot\nabla$ denotes the material derivative, and

$$u_{\mathrm{ex}} = \mathrm{Da}\left(1-\frac{\sigma_\kappa^2\mathrm{Da}}{2}\frac{\mathrm{d}f_\alpha}{\mathrm{d}x_4}\right)f_\alpha, \quad D_{\mathrm{ex}} = \frac{\sigma_\kappa^2\mathrm{Da}^2 f_\alpha^2}{2}. \tag{51}$$

Next, we note that both the effective "velocities" u_4 and "macro-dispersion" coefficients D_{44} in (42) and (49) can be written in the form that coincides with (51). Hence the PDF equation based on the LED approximation is exact for reaction

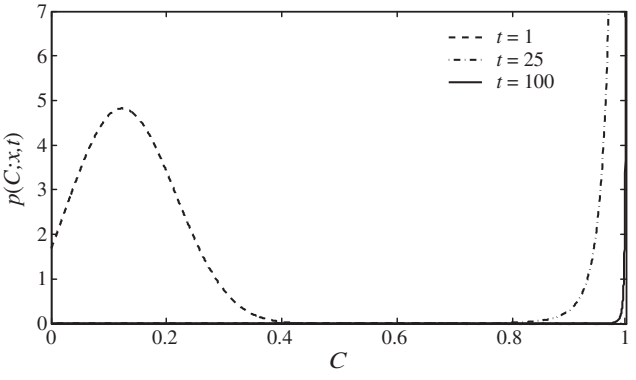

Fig. 5. Temporal evolution of the concentration PDF for the nonlinear reaction law with $\alpha = 2$, exponentially correlated reaction rate constant $\kappa(x)$ and the following choice of parameters: $\mathrm{Da} = 0.05$, $\sigma_\kappa^2 = 1$, and $da_\kappa = 1$. Snapshots are calculated at point $x = 50$.

rate constants that can be treated as white noise (an uncorrelated random field).

5. Summary and conclusions

We considered advective transport of a reactive solute in heterogeneous porous media. Uncertainty in hydraulic and transport properties of porous media was quantified by treating the relevant parameters as random fields. Under these conditions, reactive transport is described by a stochastic partial differential equation (SPDE) for concentration where the randomness is multiplicative and quenched. We derived an equation for the probability density function (PDF) of concentration by employing a closure based on the Large-Eddy-Diffusivity (LED) approximation. We used the proposed approach to compute the concentration PDFs for one-dimensional advective–reactive transport in a porous medium with uncertain reaction rate constants. Both linear and nonlinear heterogeneous reactions were considered.

Our analysis leads to the following major conclusions.

(1) The PDF equations derived in this study are capable of handling uncertainty (randomness) in both macroscopic (Darcian) velocities and reaction rate constants, and allow for an arbitrary degree of correlation between the two.
(2) By virtue of relying on the LED closure, these PDF equations are approximate. For transport with deterministic (certain) velocity and uncorrelated reaction rate constants, our PDF equations are exact for both linear and nonlinear reaction laws.
(3) The lack of spatial correlations of reaction rate constants enhances uncertainty in predictions of solute concentration.
(4) The shape of concentration PDFs is strongly influenced by the Damköhler number, which quantifies the relative importance of advection and reactions. This indicates that a functional form of concentration PDFs depends on a flow regime, boundary and initial conditions, etc., which makes the reliance on assumed PDFs problematic.
(5) The effect of nonlinearity of the dissolution reaction is to speed up the transition to equilibrium, which decreases the time interval over which predictive uncertainty is significant.

Appendix A. LED closure

Subtracting (18) from (17) yields an equation for random fluctuations Π',

$$\frac{\partial \Pi'}{\partial t} = -\nabla_{\tilde{\mathbf{x}}}\cdot(\tilde{\mathbf{v}}\Pi' + \tilde{\mathbf{v}}' p - \langle \tilde{\mathbf{v}}\Pi'\rangle). \tag{A.1}$$

Rewriting (A.1) in terms of τ and $\tilde{\mathbf{y}}$, multiplying the result with a (random) test function $\mathcal{G}(\tilde{\mathbf{x}}, \tilde{\mathbf{y}}, t-\tau)$ and integrating in space and time yield

$$\int_0^t \int_{\tilde{\Omega}} \frac{\partial \Pi'}{\partial \tau}\mathcal{G}\,\mathrm{d}\tilde{\mathbf{y}}\mathrm{d}\tau + \int_0^t \int_{\tilde{\Omega}} \nabla_{\tilde{\mathbf{y}}}\cdot(\tilde{\mathbf{v}}\Pi')\mathcal{G}\,\mathrm{d}\tilde{\mathbf{y}}\mathrm{d}\tau = -\int_0^t \int_{\tilde{\Omega}} \nabla_{\tilde{\mathbf{y}}}\cdot(\tilde{\mathbf{v}}' p - \langle \tilde{\mathbf{v}}\Pi'\rangle)\mathcal{G}\,\mathrm{d}\tilde{\mathbf{y}}\mathrm{d}\tau. \tag{A.2}$$

Integrating by parts and applying the Green's identity to the left-hand-side of (A.2) yield

$$\int_{\tilde{\Omega}} [\Pi'\mathcal{G}]_{\tau=0}^t \mathrm{d}\tilde{\mathbf{y}} - \int_0^t \int_{\tilde{\Omega}} \Pi' \frac{\partial \mathcal{G}}{\partial \tau}\mathrm{d}\tilde{\mathbf{y}}\mathrm{d}\tau + \int_0^t \int_{\tilde{\Gamma}} \tilde{\mathbf{n}}\cdot\tilde{\mathbf{v}}\Pi'\mathcal{G}\,\mathrm{d}\tilde{\mathbf{s}}\mathrm{d}\tau - \int_0^t \int_{\tilde{\Omega}} \Pi'\tilde{\mathbf{v}}\cdot\nabla_{\tilde{\mathbf{y}}}\mathcal{G}\,\mathrm{d}\tilde{\mathbf{y}}\mathrm{d}\tau = -\int_0^t \int_{\tilde{\Omega}} \nabla_{\tilde{\mathbf{y}}}\cdot(\tilde{\mathbf{v}}' \mathrm{p} - \langle \tilde{\mathbf{v}}\Pi'\rangle)\mathcal{G}\,\mathrm{d}\tilde{\mathbf{y}}\mathrm{d}\tau, \tag{A.3}$$

where $\mathbf{n}$ denotes the outward normal vector to the boundary $\tilde{\Gamma} \equiv \partial\tilde{\Omega}$ of the hyper-domain $\tilde{\Omega} \equiv \Omega \times (C_0, 1)$ or $\tilde{\Omega} \equiv \Omega \times (1, C_0)$, depending on the initial concentration value. Let $\mathcal{G}(\tilde{\mathbf{x}}, \tilde{\mathbf{y}}, t-\tau)$ be the Green's function defined as a solution of (19) subject to the initial condition $\mathcal{G}(\tilde{\mathbf{x}}, \tilde{\mathbf{y}}, t=\tau) = 0$. Then denoting $\Pi_0'(\tilde{\mathbf{y}}) = \Pi'(\tilde{\mathbf{y}}, \tau = 0)$, $\tilde{v}_n = \mathbf{n}\cdot\tilde{\mathbf{v}}$ and $\mathbf{Q} = \langle \tilde{\mathbf{v}}\Pi'\rangle$ yields an integral equation for fluctuations $\Pi'(\tilde{\mathbf{x}}, t)$,

$$\Pi' = -\int_0^t \int_{\tilde{\Omega}} \nabla_{\tilde{\mathbf{y}}}\cdot(\tilde{\mathbf{v}}' p - \mathbf{Q})\mathcal{G}\,\mathrm{d}\tilde{\mathbf{y}}\mathrm{d}\tau + \int_{\tilde{\Omega}} \Pi_0'\mathcal{G}(\tilde{\mathbf{x}}, \tilde{\mathbf{y}}, t)\mathrm{d}\tilde{\mathbf{y}} - \int_0^t \int_{\tilde{\Gamma}} \tilde{v}_n \Pi'\mathcal{G}\,\mathrm{d}\tilde{\mathbf{s}}\mathrm{d}\tau. \tag{A.4}$$

Recalling that $\tilde{\nabla}\cdot\tilde{\mathbf{v}} = \mathrm{Da}df_\kappa / \mathrm{d}x_4$, this gives

$$\Pi'(\tilde{\mathbf{x}}, t) = -\int_0^t \int_{\tilde{\Omega}} \left(\mathcal{G}\tilde{\mathbf{v}}'\cdot\nabla_{\tilde{\mathbf{y}}} p + \mathrm{Da}\frac{df_\kappa'}{dy_4} p\mathcal{G} - \mathcal{G}\nabla_{\tilde{\mathbf{y}}}\cdot\mathbf{Q}\right)\mathrm{d}\tilde{\mathbf{y}}\mathrm{d}\tau + \int_{\tilde{\Omega}} \Pi_0'\mathcal{G}(\tilde{\mathbf{x}}, \tilde{\mathbf{y}}, t)\mathrm{d}\tilde{\mathbf{y}} - \int_0^t \int_{\tilde{\Gamma}} \tilde{v}_n\Pi'\mathcal{G}\,\mathrm{d}\tilde{\mathbf{s}}\mathrm{d}\tau. \tag{A.5}$$

Multiplying (A.5) with $\tilde{\mathbf{v}}'(\mathbf{x})$ and taking the ensemble mean, while accounting for the statistical independence of the driving forces, give an integral equation for the components of the vector $\mathbf{Q}(\tilde{\mathbf{x}}, t)$,

$$Q_i = -\int_0^t \int_{\tilde{\Omega}} \left(\langle \mathcal{G}\tilde{v}_i'(\tilde{\mathbf{x}})\tilde{v}_j'(\tilde{\mathbf{y}})\rangle \frac{\partial p}{\partial \tilde{y}_j} + \mathrm{Da}\langle \mathcal{G}\tilde{v}_i'(\tilde{\mathbf{x}})\frac{df_\kappa'}{dy_4}\rangle p - \langle \mathcal{G}\tilde{v}_i'(\tilde{\mathbf{x}})\rangle \frac{\partial Q_j}{\partial \tilde{y}_j}\right)\mathrm{d}\tilde{\mathbf{y}}\mathrm{d}\tau, \tag{A.6}$$

where the Einstein notation is used to indicate the summation over the repeated index j. This expression for the mixed ensemble moment $\mathbf{Q}$ is exact, but requires some approximations to be workable. First, we note that the last term in (A.6) is of the lower order than the other three terms and, hence, can be dropped, i.e.,

$$Q_i(\tilde{\mathbf{x}}, t) \approx -\int_0^t \int_{\tilde{\Omega}} \left(\langle \mathcal{G}\tilde{v}_i'(\tilde{\mathbf{x}})\tilde{v}_j'(\tilde{\mathbf{y}})\rangle \frac{\partial p}{\partial \tilde{y}_j} + \mathrm{Da}\langle \mathcal{G}\tilde{v}_i'(\tilde{\mathbf{x}})\frac{df_\kappa'}{dy_4}\rangle p\right)\mathrm{d}\tilde{\mathbf{y}}\mathrm{d}\tau. \tag{A.7}$$

To arrive at the LED approximation, we further assume that both ∇p and p vary slowly in space, so that

$$Q_i(\tilde{\mathbf{x}},t)\approx-\frac{\partial p(\tilde{\mathbf{x}},t)}{\partial \tilde{x}_j}\int_0^t\int_{\tilde{\Omega}}\langle \mathcal{G}\tilde{v}'_i(\tilde{\mathbf{x}})\tilde{v}'_j(\tilde{\mathbf{y}})\rangle \mathrm{d}\tilde{\mathbf{y}}\mathrm{d}\tau \qquad (A.8)$$
$$-p(\tilde{\mathbf{x}},t)\mathrm{Da}\int_0^t\int_{\tilde{\Omega}}\langle \mathcal{G}\tilde{v}'_i(\tilde{\mathbf{x}})\frac{df'_\kappa}{dy_4}\rangle \mathrm{d}\tilde{\mathbf{y}}\mathrm{d}\tau.$$

Substituting (A.8) into (18) leads to (20).

Appendix B. Green's functions

For deterministic flow velocity, $v'_i(\mathbf{x})\equiv 0$ $(i=1,2,3)$, so that the general Green's function Eq. (25) simplifies to

$$\frac{\partial G}{\partial \tau}+\mathbf{v}\cdot\nabla_{\mathbf{y}}G+\mathrm{Da}f_\alpha(y_4)\frac{\partial G}{\partial y_4}=-\delta(\mathbf{x}-\mathbf{y})\delta(x_4-y_4)\delta(t-\tau). \qquad (B.1)$$

This equation is defined for $\tau<t$, and is subject to the initial condition $G(\tilde{\mathbf{x}},\tilde{\mathbf{y}},\tau=t)=0$ and the causality principle $G(\tilde{\mathbf{x}},\tilde{\mathbf{y}},\tau>t)=0$. Setting $T\equiv t-\tau$ and recalling that $f_\alpha(y_4)\equiv -\alpha(y_4^\alpha-1)$, we obtain

$$\frac{\partial G}{\partial T}-\mathbf{v}\cdot\nabla_{\mathbf{y}}G+\alpha\mathrm{Da}(y_4^\alpha-1)\frac{\partial G}{\partial y_4}=\delta(\mathbf{x}-\mathbf{y})\delta(x_4-y_4)\delta(T), T>0 \qquad (B.2)$$

subject to $G(\tilde{\mathbf{x}},\tilde{\mathbf{y}},0)=0$ and $G(\tilde{\mathbf{x}},\tilde{\mathbf{y}},T<0)=0$. Since the Green's function G in (B.2) can be found as the product of one-dimensional Green's functions, e.g., $G(\tilde{\mathbf{x}},\tilde{\mathbf{y}},T)=G_{3d}(\mathbf{x},\mathbf{y},T)G_4(x_4,y_4,T)$, we start by solving

$$\frac{\partial G_4}{\partial T}+\alpha\mathrm{Da}(y_4^\alpha-1)\frac{\partial G_4}{\partial y_4}=\delta(x_4-y_4)\delta(T),\ T>0. \qquad (B.3)$$

The equation for characteristics in (B.3) is

$$\frac{\mathrm{d}y_4}{\mathrm{d}T}=\alpha\mathrm{Da}(y_4^\alpha-1),\ y_4(0)=\xi. \qquad (B.4)$$

Along these characteristics,

$$\frac{\mathrm{d}G_4}{\mathrm{d}T}=\delta[x_4-y_4(\xi,T)]\delta(T),\ G_4(x_4,\xi,0)=0. \qquad (B.5)$$

For an arbitrary α, the solution of (B.4) is given by

$${}_2F_1\left[\frac{1}{\alpha},1;1+\frac{1}{\alpha},y_4^\alpha\right]y_4-{}_2F_1\left[\frac{1}{\alpha},1;1+\frac{1}{\alpha},\xi^\alpha\right]\xi=\alpha\mathrm{Da}T, \qquad (B.6)$$

where ${}_2F_1$ is a hypergeometric function. The solution of (B.5) is

$$G_4(x_4,\xi,T)=\int_0^T\delta[x_4-y_4(\xi,T')]\delta(T')\mathrm{d}T'=\delta[x_4-y_4(\xi,0)]$$
$$=\delta(x_4-\xi). \qquad (B.7)$$

The Green's function $G_{3d}(\mathbf{x},\mathbf{y},T)$ is a solution of

$$\frac{\partial G_{3d}}{\partial T}-\mathbf{v}\cdot\nabla_{\mathbf{y}}G_{3d}=\delta(\mathbf{x}-\mathbf{y})\delta(T),\ T>0. \qquad (B.8)$$

Using the method of characteristics to solve (B.8) for constant $\mathbf{v}$ leads to

$$G_{3d}(\mathbf{x},\mathbf{y},T)=\delta(\mathbf{x}-\mathbf{y}-\mathbf{v}T),\ T>0. \qquad (B.9)$$

The complete Green's function is given by the product of (B.9) and (B.7),

$$G=[1-\mathcal{H}(\tau-t)]\delta(x-y-(t-\tau))\delta(x_4(\tau)-\xi), \qquad (B.10)$$

where the constant velocity $\mathbf{v}$ is aligned with the x_1 coordinate (denoted forthwith by x) and set to $v=1$, $\mathcal{H}(\cdot)$ is the Heaviside function and ξ is a solution of (B.6) with $T\equiv t-\tau$.

Appendix B.1. Linear reaction, $\alpha=1$

For $\alpha=1$, (B.6) simplifies to

$$y_4(\xi,T)=1+(\xi-1)\mathrm{e}^{\mathrm{Da}T}. \qquad (B.11)$$

Using (B.11) to eliminate ξ in favor of y_4 and T, and substituting the result into (B.7), we obtain

$$G_4(x_4,y_4,T)=\delta\left[x_4-(y_4-1)\mathrm{e}^{-\mathrm{Da}T}-1\right],\ T>0. \qquad (B.12)$$

Substituting (B.12) into (B.10) gives an expression for the Green's function,

$$G=[1-\mathcal{H}(\tau-t)]\delta[x-y-(t-\tau)]\delta\left[x_4-(y_4-1)^{-\mathrm{Da}(t-\tau)}-1\right]. \qquad (B.13)$$

Appendix B.2. Nonlinear reaction, $\alpha=2$

For $\alpha=2$, (B.6) reduces to

$$y_4(\xi,T)=2\left(1-\frac{\xi-1}{\xi+1}e^{4\mathrm{Da}T}\right)^{-1}-1. \qquad (B.14)$$

Using (B.14) to eliminate ξ in favor of y_4 and T, and substituting the result into (B.7), we arrive at

$$G_4(x_4,y_4,T)=\delta\left[x_4-2\left(\frac{y_4+1}{y_4-1}\mathrm{e}^{4\mathrm{Da}T}-1\right)^{-1}-1\right],\ T>0. \qquad (B.15)$$

Substituting (B.15) into (B.10) gives an expression for the Green's function,

$$G=\mathcal{H}(T)\delta[x-y-T]\delta\left[x_4-2\left(\frac{y_4+1}{y_4-1}\mathrm{e}^{4\mathrm{Da}T}-1\right)^{-1}-1\right], \qquad (B.16)$$

where $T=t-\tau$.

Appendix C. Dispersion coefficient and effective velocity

Appendix C.1. Linear reaction

Substituting (B.13) into (31) gives

$$D_{44} = \mathrm{Da}^2(x_4-1)\int_0^t \int_{\tilde{\Omega}} C_\kappa(x,y)(y_4-1) \times\delta[x-y-(t-\tau)]\delta\left[x_4-(y_4-1)^{-\mathrm{Da}(t-\tau)}-1\right]\mathrm{d}\tilde{\mathbf{y}}\mathrm{d}\tau. \tag{C.1}$$

Denoting $T=t-\tau$, recalling that $\Omega_4\equiv[0,1]$, and integrating over y yield

$$D_{44} = \mathrm{Da}^2(x_4-1)\int_0^t C_\kappa(x,x-T)\int_0^1 (y_4-1) \times\delta\left[x_4-(y_4-1)e^{-\mathrm{Da}T}-1\right]\mathrm{d}y_4\mathrm{d}T. \tag{C.2}$$

To evaluate the integral over y_4, we note that for any function $g(z)$,

$$\delta[g(z)] = \sum_i \frac{\delta(z-z_i)}{|g'(z_i)|}, \tag{C.3}$$

where z_i are roots of the equation $g(z)=0$. This leads to

$$D_{44} = \mathrm{Da}^2(x_4-1)\int_0^t C_\kappa(x,x-T)\mathrm{e}^{\mathrm{Da}T}\int_0^1 (y_4-1) \times\delta\left[y_4-1-(x_4-1)\mathrm{e}^{\mathrm{Da}T}\right]\mathrm{d}y_4\mathrm{d}T. \tag{C.4}$$

This integral is not zero as long as $1+(x_4-1)\mathrm{e}^{\mathrm{Da}T}\in[0,1]$. Since $x_4\in[0,1]$ and $y(T)=1+(x_4-1)\mathrm{e}^{\mathrm{Da}T}$ is a decreasing function, we have to consider two cases.

Case 1. $y_4(T=t)=1+(x_4-1)\mathrm{e}^{\mathrm{Da}t}\geq 0$. Then

$$\begin{aligned} D_{44} &= \mathrm{Da}^2(x_4-1)\int_0^t C_\kappa(x,x-T)\mathrm{e}^{\mathrm{Da}T}\int_0^{x_4}(y_4-1) \times\delta\left[y_4-1-(x_4-1)\mathrm{e}^{\mathrm{Da}T}\right]\mathrm{d}y_4\mathrm{d}T \\ &= \mathrm{Da}^2(x_4-1)^2\int_0^t C_\kappa(x,x-T)\mathrm{e}^{2\mathrm{Da}T}\mathrm{d}T. \end{aligned} \tag{C.5}$$

Case 2. $y_4(T=t)=1+(x_4-1)\mathrm{e}^{\mathrm{Da}t}<0$. Then

$$\begin{aligned} D_{44} &= \mathrm{Da}^2(x_4-1)\int_0^{t_*} C_\kappa(x,x-T)\mathrm{e}^{\mathrm{Da}T}\int_0^{x_4}(y_4-1) \times\delta\left[y_4-1-(x_4-1)\mathrm{e}^{\mathrm{Da}T}\right]\mathrm{d}y_4\mathrm{d}T \\ &= \mathrm{Da}^2(x_4-1)^2\int_0^{t_*} C_\kappa(x,x-T)\mathrm{e}^{2\mathrm{Da}T}\mathrm{d}T, \end{aligned} \tag{C.6}$$

where

$$y_4(T=t_*)=0 \quad\Rightarrow\quad t_* = \frac{1}{\mathrm{Da}}\ln\frac{1}{1-x_4}. \tag{C.7}$$

This gives (38).

Substituting (B.13) into the second equation in (27) gives

$$u_4 = \mathrm{Da}(1-x_4)-\mathrm{Da}^2(x_4-1)\int_0^1 C_\kappa(x,x-T) \times\int_0^1\delta\left[x_4-(y_4-1)e^{-\mathrm{Da}T}-1\right]\mathrm{d}y_4\mathrm{d}T. \tag{C.8}$$

Following the reasoning used to compute the dispersion coefficient D_{44}, we have to consider two cases while computing this integral.

Case 1. $y_4(T=t)=1+(x_4-1)\mathrm{e}^{\mathrm{Da}t}\geq 0$. Then

$$\begin{aligned} u_4 &= \mathrm{Da}(1-x_4)-\mathrm{Da}^2(x_4-1)\int_0^t C_\kappa(x,x-T)\mathrm{e}^{\mathrm{Da}T}\int_0^{x_4} \times\delta\left[y_4-1-(x_4-1)\mathrm{e}^{\mathrm{Da}T}\right]dy_4\mathrm{d}T \\ &= \mathrm{Da}(1-x_4)-\mathrm{Da}^2(x_4-1)\int_0^t C_\kappa(x,x-T)\mathrm{e}^{\mathrm{Da}T}\mathrm{d}T. \end{aligned} \tag{C.9}$$

Case 2. $y_4(T=t)=1+(x_4-1)\mathrm{e}^{\mathrm{Da}t}<0$. Then

$$\begin{aligned} u_4 &= \mathrm{Da}(1-x_4)-\mathrm{Da}^2(x_4-1)\int_0^{t_*} C_\kappa(x,x-T)\mathrm{e}^{\mathrm{Da}T} \times\int_0^{x_4}\delta\left[y_4-1-(x_4-1)\mathrm{e}^{\mathrm{Da}T}\right]\mathrm{d}y_4\mathrm{d}T \\ &= \mathrm{Da}(1-x_4)-\mathrm{Da}^2(x_4-1)\int_0^{t_*} C_\kappa(x,x-T)\mathrm{e}^{\mathrm{Da}T}\mathrm{d}T. \end{aligned} \tag{C.10}$$

This gives (44).

Appendix C.2. Nonlinear reaction, $\alpha=2$

Substituting (B. 16) into (31) gives

$$D_{44} = 4\mathrm{Da}^2\left(x_4^2-1\right)\int_0^t C_\kappa(x,x-T)\int_0^1\left(y_4^2-1\right)\delta[g(y_4,T)]\mathrm{d}y_4\mathrm{d}T, \tag{C.11}$$

where

$$g(y_4,T) = x_4-2\left(\frac{y_4+1}{y_4-1}\mathrm{e}^{4\mathrm{Da}T}-1\right)^{-1}-1. \tag{C.12}$$

To evaluate the integral over y_4, we observe that a root y_* of the equation $g(y_4,T)=0$ is

$$y_* = 1+2\left(\frac{x_4+1}{x_4-1}\mathrm{e}^{-4\mathrm{Da}T}-1\right)^{-1}. \tag{C.13}$$

Then, according to (C.3),

$$\delta[g(y_4,T)] = \frac{4}{(x_4-1)^2}\mathrm{e}^{-4\mathrm{Da}T}\left(\frac{x_4+1}{x_4-1}\mathrm{e}^{-4\mathrm{Da}T}-1\right)^{-2}\delta(y_4-y_*) \tag{C.14}$$

and (C.11) becomes

$$D_{44} = 16\mathrm{Da}^2 \frac{x_4+1}{x_4-1} \int_0^t C_\kappa(x, x-T) \mathrm{e}^{-4\mathrm{Da}T} \left(\frac{x_4+1}{x_4-1} \mathrm{e}^{-4\mathrm{Da}T} - 1 \right)^{-2} \times \int_0^1 \left(y_4^2 - 1 \right) \delta(y_4 - y_*) \mathrm{d}y_4 \mathrm{d}T. \tag{C.15}$$

This integral is not zero as long as $y_i \in [0,1]$. Again, two cases are possible, depending on the sign of $y_*(T=t)$. In other words, we have to consider two cases, $t \le t_*$ or $t > t_*$, where

$$t_* = \frac{1}{4\mathrm{Da}} \ln \frac{1+x_4}{1-x_4}. \tag{C.16}$$

Case 1. $t \le t_*$. It follows from (C.15) that

$$\begin{aligned} D_{44} &= 16\mathrm{Da}^2 \frac{x_4+1}{x_4-1} \int_0^t C_\kappa(x, x-T) \mathrm{e}^{-4\mathrm{Da}T} \left(\frac{x_4+1}{x_4-1} \mathrm{e}^{-4\mathrm{Da}T} - 1 \right)^{-2} \\ &\times \int_0^1 \left(y_4^2 - 1 \right) \delta(y_4 - y_*) \mathrm{d}y_4 \mathrm{d}T \\ &= 16\mathrm{Da}^2 \frac{x_4+1}{x_4-1} \int_0^t C_\kappa(x, x-T) \mathrm{e}^{-4\mathrm{Da}T} \left(\frac{x_4+1}{x_4-1} \mathrm{e}^{-4\mathrm{Da}T} - 1 \right)^{-2} \left(y_*^2 - 1 \right) \mathrm{d}T. \end{aligned} \tag{C.17}$$

Case 2. $t > t_*$. Then

$$\begin{aligned} D_{44} &= 16\mathrm{Da}^2 \frac{x_4+1}{x_4-1} \int_0^{t_*} C_\kappa(x, x-T) \mathrm{e}^{-4\mathrm{Da}T} \left(\frac{x_4+1}{x_4-1} \mathrm{e}^{-4\mathrm{Da}T} - 1 \right)^{-2} \\ &\times \int_0^1 \left(y_4^2 - 1 \right) \delta(y_4 - y_*) \mathrm{d}y_4 \mathrm{d}T \\ &= 16\mathrm{Da}^2 \frac{x_4+1}{x_4-1} \int_0^{t_*} C_\kappa(x, x-T) \mathrm{e}^{-4\mathrm{Da}T} \left(\frac{x_4+1}{x_4-1} \mathrm{e}^{-4\mathrm{Da}T} - 1 \right)^{-2} \left(y_*^2 - 1 \right) \mathrm{d}T. \end{aligned} \tag{C.18}$$

Substitution of (C. 13) into (C.17) and (C.18) leads to (46).

The effective velocity u_4 is computed by substituting (B. 16) into (27),

$$u_4 = \mathrm{Da} f_2 + 4\mathrm{Da}^2 f_2 \int_0^t C_\kappa(x, x-T) \int_0^1 y_4 \times \delta \left[x_4 - 2 \left(\frac{y_4+1}{y_4-1} \mathrm{e}^{4\mathrm{Da}T} - 1 \right)^{-1} - 1 \right] \mathrm{d}y_4 \mathrm{d}T. \tag{C.19}$$

Replacing the delta function in (C.19) with (C.14) leads to

$$u_4 = \mathrm{Da} f_2 + 16\mathrm{Da}^2 \frac{f_2}{(x_4-1)^2} \int_0^t C_\kappa(x, x-T) \mathrm{e}^{-4\mathrm{Da}T} \left(\frac{x_4+1}{x_4-1} \mathrm{e}^{-4\mathrm{Da}T} - 1 \right)^{-2} \times \int_0^1 y_4 \delta(y_4 - y_*) \mathrm{d}y_4 \mathrm{d}T. \tag{C.20}$$

Computing the integral over y_4, while accounting for the requirement that $y \in [0,1]$, we obtain

$$u_4 = \mathrm{Da} f_2 + \frac{16\mathrm{Da}^2 f_2}{(x_4-1)^2} \begin{cases} \int_0^t C_\kappa(x, x-T) \mathrm{e}^{-4\mathrm{Da}T} \left(\frac{x_4+1}{x_4-1} \mathrm{e}^{-4\mathrm{Da}T} - 1 \right)^{-2} y_* \mathrm{d}T & t \le t_* \\ \int_0^{t_*} C_\kappa(x, x-T) \mathrm{e}^{-4\mathrm{Da}T} \left(\frac{x_4+1}{x_4-1} \mathrm{e}^{-4\mathrm{Da}T} - 1 \right)^{-2} y_* \mathrm{d}T & t > t_* \end{cases}. \tag{C.21}$$

Recalling the definitions of y and f_2, we obtain (47).

References

Battiato, I., Tartakovsky, D.M., 2011. Regimes of applicability of macroscopic descriptions of reactive transport in porous media. J. Contam. Hydrol. 120–121 (C), 18–26 (this issue).

Bellin, A., Rinaldo, A., Bosma, W.J.P., van der Zee, S.E.A.T.M., Rubin, Y., 1993. Linear equilibrium adsorbing solute transport in physically and chemically heterogeneous porous formations 1. Analytical solutions. Water Resour. Res. 29 (12), 4019–4030.

Bolster, D., Barahona, M., Dentz, M., Fernandez-Garcia, D., Sanchez-Vila, X., Trinchero, P., Valhondo, C., Tartakovsky, D.M., 2009. Probabilistic risk analysis of groundwater remediation strategies. Water Resour. Res. 45, W06413 doi:10.1029/2008wr007551.

Broyda, S., Dentz, M., Tartakovsky, D.M., 2010. Probability density functions for advective-reactive transport in radial flow. Stoch. Environ. Res. Risk Assess. doi:10.1007/s00477–010–0401–4.

Cushman, J.H., 1997. The physics of fluids in hierarchical porous media: Angstroms to miles. Kluwer Academic Pub, New York.

Cushman, J.H., Hu, B.X., Deng, F.W., 1995. Nonlocal reactive transport with physical and chemical heterogeneity: localization errors. Water Resour. Res. 31 (9), 2219–2237.

Cvetkovic, V., Selroos, J.O., Cheng, H., 1999. Transport of reactive tracers in rock fractures. J. Fluid Mech. 378, 335–356.

Dagan, G., 1989. Flow and transport in porous formations. Springer-Verlag, New York.

Dagan, G., Neuman, S.P. (Eds.), 1997. Subsurface flow and transport: A stochastic approach Cambridge, New York.

Dentz, M., Tartakovsky, D.M., 2008. Self-consistent four-point closure for transport in steady random flows. Phys. Rev. E 77 (6), 066307. doi:10.1103/PhysRevE.77.066307.

Foo, J., Karniadakis, G.E., 2010. Multi-element probabilistic collocation method in high dimensions. J. Comput. Phys. 229 (5), 1536–1557.

Frisch, U., 1968. Wave propagation in random media. In: Bharucha-Reid, A.T. (Ed.), Probabilistic methods in applied mathematics, vol. 1. Academic Press, New York, pp. 75–198.

Gelhar, L.W., 1993. Stochastic subsurface hydrology. Prentice Hall, New Jersey.

Ginn, T.R., Murphy, E.M., Chilakapati, A., Seeboonruang, U., 2001. Stochastic–convective transport with nonlinear reaction and mixing: application to intermediate-scale experiments in aerobic biodegradation in saturated porous media. J. Contam. Hydrol. 48 (1–2), 121–149.

Jarman, K.D., Tartakovsky, A.M., 2008. Divergence of solutions to solute transport moment equations. Geophys. Res. Lett. 35 (15), 30–34.

Kechagia, P.E., Tsimpanogiannis, I.N., Yortsos, Y.C., Lichtner, P.C., 2002. On the upscaling of reaction-transport processes in porous media with fast or finite kinetics. Chem. Eng. Sci. 57 (13), 2565–2577.

Kraichnan, R.H., 1965. Lagrangian-history closure approximation for turbulence. Phys. Fluids 8 (4), 575–598.

Kraichnan, R.H., 1987. Eddy viscosity and diffusivity: exact formulas and approximations. Complex Syst. 1, 805–820.

Lichtner, P.C., Tartakovsky, D.M., 2003. Upscaled effective rate constant for heterogeneous reactions. Stoch. Environ. Res. Risk Assess. 17 (6), 419–429.

Lin, G., Tartakovsky, A.M., 2009. An efficient, high-order probabilistic collocation method on sparse grids for three-dimensional flow and solute transport in randomly heterogeneous porous media. Adv. Water Resour. 32 (5), 712–722.

Neuman, S.P., 1993. Eulerian–Lagrangian theory of transport in space–time nonstationary velocity fields: exact nonlocal formalism by conditional moments and weak approximation. Water Resour. Res. 29 (3), 633–645.

Neuman, S.P., Tartakovsky, D.M., 2009. Perspective on theories of anomalous transport in heterogeneous media. Adv. Water Resour. 32 (5), 670–680.
Pope, S.B., 1981. Transport equation for the joint probability density function of velocity and scalars in turbulent flow. Phys. Fluids 24 (4), 588–596.
Pope, S.B., 2000. Turbulent flows. Cambridge University Press, Cambridge, UK.
Severino, G., Monetti, V., Santini, A., Toraldo, G., 2006. Unsaturated transport with linear kinetic sorption under unsteady vertical flow. Transp. Porous Media 63 (1), 147–174.
Shvidler, M., Karasaki, K., 2003. Probability density functions for solute transport in random field. Transp. Porous Media 50 (3), 243–266.
Simmons, C.S., Ginn, T.R., Wood, B.D., 1995. Stochastic–convective transport with nonlinear reaction: mathematical framework. Water Resour. Res. 31 (11), 2675–2688.
Tartakovsky, A.M., Meakin, P., Scheibe, T.D., West, R.M.E., 2007a. Simulation of reactive transport and precipitation with smoothed particle hydrodynamics. J. Comput. Phys. 222, 654–672.
Tartakovsky, A.M., Redden, G., Lichtner, P.C., Scheibe, T.D., Meakin, P., 2008. Mixing-induced precipitation: experimental study and multi-scale numerical analysis. Water Resour. Res. 44, W06S04 doi:10.1029/2006WR005725.
Tartakovsky, A.M., Tartakovsky, D.M., Scheibe, T.D., Meakin, P., 2007b. Hybrid simulations of reaction–diffusion systems in porous media. SIAM J. Sci. Comput. 30 (6), 2799–2816.
Tartakovsky, D.M., 2007. Probabilistic risk analysis in subsurface hydrology. Geophys. Res. Lett. 34, L05404 doi:10.1029/2007GL029245.
Tartakovsky, D.M., Dentz, M., Lichtner, P.C., 2009. Probability density functions for advective–reactive transport in porous media with uncertain reaction rates. Water Resour. Res. 45, W07414 doi:10.1029/2008WR007383.
Winter, C.L., Newman, C.M., Neuman, S.P., 1984. A perturbation expansion for diffusion in a random velocity field. SIAM J. Appl. Math. 44 (2), 411–424.
Winter, C.L., Tartakovsky, D.M., 2008. A reduced complexity model for probabilistic risk assessment of groundwater contamination. Water Resour. Res. 44, W06501 doi:10.1029/2007WR006599.
Xiu, D., Tartakovsky, D.M., 2004. A two-scale non-perturbative approach to uncertainty analysis of diffusion in random composites. J. Multiscale Model. Simul. 2 (4), 662–674.
Xiu, D., Tartakovsky, D.M., 2006. Numerical methods for differential equations in random domains. SIAM J. Sci. Comput. 28 (3), 1167–1185.